© 2015. Published by The Company of Biologists Ltd | Journal of Cell Science (2015) 128, 2565 doi:10.1242/jcs.175323

CORRECTION

RILP regulates vacuolar ATPase through interaction with the V1G1 subunit

Maria De Luca, Laura Cogli, Cinzia Progida, Veronica Nisi, Roberta Pascolutti, Sara Sigismund, Pier Paolo Di Fiore and Cecilia Bucci

There was an error published in *J. Cell Sci.* **127**, 2697-2708.

In Fig. 2, the V1C1 western blot was inadvertently duplicated in panels A and B. The V1C1 western blot has been replaced with the correct image in panel B in the figure shown below. There are no changes to the figure legend, which is accurate. This error does not affect the conclusions of the study.

The authors apologise to the readers for any confusion that this error might have caused.

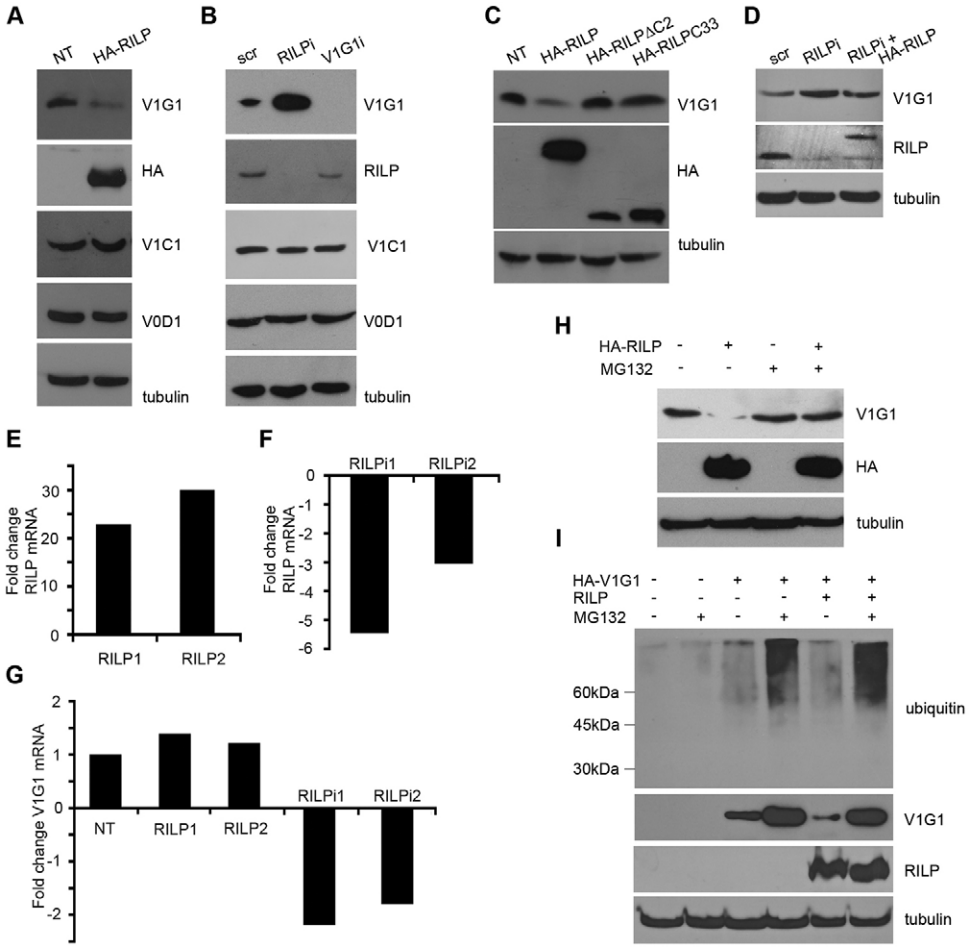

Fig. 2. RILP modulates V1G1 abundance in HeLa cells through ubiquitylation-dependent proteasomal degradation. (A) Lysates of control HeLa cells (NT) or cells expressing HA–RILP were subjected to western blot analysis using primary antibodies against V1G1, HA, V1C1, V0D1 and tubulin. (B) Cells treated with control siRNA (scr), RILP-specific siRNA (RILPi) or V1G1-specific siRNA (V1G1i) were subjected to western blot analysis using primary antibodies against V1G1, RILP, V1C1, V0D1 and tubulin. (C) Lysates of control HeLa cells or cells expressing HA–RILP, HA–RILPΔC2 or HA–RILPC33 were subjected to western blot analysis using anti-V1G1, anti-HA and anti-tubulin antibodies. (D) Cells treated with control siRNA or RILP-specific siRNA and transfected with HA–RILP, as indicated, were subjected to western blot analysis using anti-V1G1, anti-RILP and anti-tubulin antibodies. (E–G) Real-time PCR was performed on control HeLa cells, or cells expressing HA–RILP (RILP1 and RILP2) or silenced for RILP (RILPi1 and RILPi2), and the amount of RILP (E,F) or of V1G1 (G) was quantified relative to the control GAPDH RNA transcript. (H) Control cells or cells expressing HA–RILP, as indicated, were either untreated or treated with the proteasomal inhibitor MG132. Lysates were then subjected to western blot analysis with antibodies against V1G1, HA and tubulin. (I) Control cells or cells transfected with HA–V1G1 and RILP, as indicated, were either untreated or treated with MG132. Lysates were subjected to western blot analysis using antibodies against RILP, V1G1 and tubulin, and to immunoprecipitation using an anti-HA antibody. Immunoprecipitates were subjected to western blot analysis using an anti-ubiquitin antibody.

© 2014. Published by The Company of Biologists Ltd | Journal of Cell Science (2014) 127, 2697–2708 doi:10.1242/jcs.142604

RESEARCH ARTICLE

RILP regulates vacuolar ATPase through interaction with the V1G1 subunit

Maria De Luca[1], Laura Cogli[1], Cinzia Progida[1,*], Veronica Nisi[1], Roberta Pascolutti[2], Sara Sigismund[2], Pier Paolo Di Fiore[2] and Cecilia Bucci[1,‡]

ABSTRACT

Rab-interacting lysosomal protein (RILP) is a downstream effector of the Rab7 GTPase. GTP-bound Rab7 recruits RILP to endosomal membranes and, together, they control late endocytic traffic, phagosome and autophagosome maturation and are responsible for signaling receptor degradation. We have identified, using different approaches, the V1G1 (officially known as ATP6V1G1) subunit of the vacuolar ATPase (V-ATPase) as a RILP-interacting protein. V1G1 is a component of the peripheral stalk and is fundamental for correct V-ATPase assembly. We show here that RILP regulates the recruitment of V1G1 to late endosomal and lysosomal membranes but also controls V1G1 stability. Indeed, we demonstrate that V1G1 can be ubiquitylated and that RILP is responsible for proteasomal degradation of V1G1. Furthermore, we demonstrate that alterations in V1G1 expression levels impair V-ATPase activity. Thus, our data demonstrate for the first time that RILP regulates the activity of the V-ATPase through its interaction with V1G1. Given the importance of V-ATPase in several cellular processes and human diseases, these data suggest that modulation of RILP activity could be used to control V-ATPase function.

KEY WORDS: RILP, Vacuolar ATPase, Rab7, V1G1, Ubiquitin

INTRODUCTION

Vacuolar-type H^+ ATPases (V-ATPases) are large multi-subunit complexes that control the acidity of intracellular compartments, and they are also responsible for proton transport across the plasma membrane and thus for acidification of the extracellular environment (Forgac, 2007; Sun-Wada et al., 2004; Toei et al., 2010). They are proton pumps that are conserved in all eukaryotes, and they are organized into two domains that constitute a rotary machine (Cipriano et al., 2008; Kane, 2006; Kane and Smardon, 2003). V0 is the integral transmembrane domain responsible for proton translocation, whereas V1 is the peripheral domain located on the cytoplasmic side of the membrane, and it is responsible for ATP hydrolysis, thus providing energy to pump the protons (Cipriano et al., 2008; Kane, 2006; Kane and Smardon, 2003). Accurate control of the pH of intracellular organelles and the extracellular milieu is fundamental for many cellular processes, including the processing and degradation of macromolecules in secretory and digestive compartments, coupled transport of small molecules such as neurotransmitters, sperm maturation and osteoclast function. Defects in acidification have been recently recognized as an important cause of several severe human diseases, such as renal tubule acidosis, osteopetrosis, defects in sperm maturation and diabetes (Casey et al., 2010; Marshansky and Futai, 2008). In addition, V-ATPase activity regulates membrane fusion, early-to-late endosomal trafficking and neurosecretion (El Far and Seagar, 2011; Hurtado-Lorenzo et al., 2006; Qiu, 2012). These proton pumps are required for invasion by endothelial cells during angiogenesis. Importantly, V-ATPases also contribute to the invasive properties of tumor cells (Forgac, 2007; Sennoune et al., 2004b). In tumor cells, V-ATPases are targeted to the plasma membrane and acidify the extracellular environment, activating lysosomal enzymes that are responsible for the degradation of the extracellular matrix. Thus, V-ATPases are directly involved in invasiveness and are now considered a very promising target in metastasis (Forgac, 2007).

The reversible dissociation of the V-ATPase complex into the V1 and V0 domains represents a fundamental control mechanism of V-ATPase function that acts to vary the rate of proton pumping (Forgac, 2007). However, the reversible dissociation of single subunits within the V1 and V0 domains has also been reported to regulate V-ATPase activity (Qi et al., 2007). A complex named RAVE (regulator of ATPase of vacuoles and endosomes) regulates the assembly of the pumps (Smardon et al., 2002). In addition, extracellular pH also tightly regulates V-ATPase activity and assembly (Diakov and Kane, 2010).

Rab-interacting lysosomal protein (RILP) is an effector of the small GTPase Rab7 (Cantalupo et al., 2001; Bucci et al., 1988; Chavrier et al., 1990). Rab proteins localize to the cytosolic side of intracellular organelles and regulate membrane traffic (Aloisi and Bucci, 2013; Bucci and Chiariello, 2006; Stenmark, 2009). Rab7, in its active GTP-bound form, recruits RILP to the membrane and together they control trafficking to late endosomes and lysosomes in the endocytic route (Bucci et al., 2000; Cantalupo et al., 2001; Jordens et al., 2001). Furthermore, RILP is involved in the biogenesis of multivesicular bodies (MVBs) (Progida et al., 2007; Progida et al., 2006).

Using the yeast two-hybrid system, we have identified the V1G1 (officially known as ATP6V1G1) subunit of V-ATPase as a RILP-interacting protein. Our data indicate that RILP, through its direct interaction with V1G1, regulates the function of V-ATPase. Thus, we have discovered a new regulatory mechanism of V-ATPase function, and, given the involvement of V-ATPase in several human diseases, these data suggest that RILP could

[1]Department of Biological and Environmental Sciences and Technologies, (DiSTeBA) University of Salento, Via Provinciale Monteroni 165, 73100 Lecce, Italy. [2]IFOM, Fondazione Istituto FIRC di Oncologia Molecolare, Via Adamello 16, 20139, Milan, Italy.
*Present address: Centre for Immune Regulation, Department of Molecular Biosciences, University of Oslo, 0316 Oslo, Norway.

‡Author for correspondence (cecilia.bucci@unisalento.it)

Received 11 September 2013; Accepted 7 March 2014

Journal of Cell Science

Journal of Cell Science (2014) 127, 2697–2708 doi:10.1242/jcs.142604

become a useful target for the development of effective therapeutic interventions.

RESULTS

RILP interacts with the V1G1 subunit of the V-ATPase

A yeast two-hybrid screen was used to identify proteins that interact with RILP. A Gal4-binding-domain–RILP fusion construct was encoded in the pGBKT7 vector and was used in the screen to identify putative interactors. The construct was used to screen a liver cDNA library encoding proteins as C-terminal fusions with the transcriptional-activation domain of Gal4 in the pACT2 vector. Of 1.3×10^6 primary transformants, 27 were His^+LacZ^+ and encoded true positives that did not activate transcription in the presence of a non-specific test bait. Seven transformants encoded the entire V1G1 subunit of the vacuolar ATPase. The interaction was revealed by the growth of yeast cells expressing RILP and V1G1 on synthetic medium lacking histidine and adenine. In the two-hybrid system, the interaction was specific as the yeasts expressing V1G1 together with Rab7 were not able to grow without histidine or without histidine and adenine (supplementary material Fig. S1A). These results were confirmed using the other reporter gene, β-galactosidase (supplementary material Fig. S1B). Using a β-galactosidase quantitative liquid assay, we confirmed the interaction between RILP and V1G1, and established, using previously described RILP deletion mutant constructs (Colucci et al., 2005a), that V1G1 binds to the N-terminal half of RILP (supplementary material Fig. S1).

To confirm the results obtained with the two-hybrid screen we investigated whether the two proteins were able to co-immunoprecipitate. HeLa cells were transfected with constructs expressing HA-tagged RILP, V1G1 or both, or were not transfected, and immunoprecipitation was performed using an anti-HA resin. The presence of immunoprecipitates of HA-tagged RILP containing the V1G1 subunit of V-ATPase confirmed the interaction (Fig. 1A). In addition, by overexpressing V1G1, RILP, RILPC33 (a truncated mutant lacking the N-terminal half of the protein) and RILPΔC2 (a truncated mutant lacking the C-terminal half of the protein), we established that V1G1 could be immunoprecipitated by RILPΔC2 but not by RILPC33 (Fig. 1B), thus confirming the data obtained with the two-hybrid system, which indicated that V1G1 binds to the N-terminal half of RILP (supplementary material Fig. S1). In order to verify the physiological significance of the interaction, we also demonstrated co-immunoprecipitation of endogenous RILP and V1G1 using a crosslink immunoprecipitation kit as described in Materials and Methods (Fig. 1C).

Subsequently, to check whether the interaction was direct, we purified bacterially expressed GST, GST-tagged RILP, GST-tagged RILPC33 and His-tagged V1G1. Glutathione resin alone or bound to GST, GST–RILP or GST–RILPC33 was incubated with His-tagged V1G1. The V1G1 subunit specifically bound only to GST-tagged RILP, demonstrating a direct interaction between V1G1 and RILP (Fig. 1D). Taken together, these results demonstrate that RILP is able to interact directly with the V1G1 subunit of the vacuolar ATPase, and this interaction is physiologically relevant.

RILP interacts simultaneously with V1G1 and $p150^{Glued}$

RILP is able also to interact directly with the C-terminal domain of $p150^{Glued}$ (also known as DCTN1), a component of the dynactin projecting arm domain, controlling transport of Rab7-positive organelles towards the cell center (Cantalupo et al., 2001; Jordens et al., 2001; Johansson et al., 2007; Harrison et al., 2003). Because acidification of endosomes correlates with their translocation towards the microtubule organizing center, we investigated whether the interactions of RILP with $p150^{Glued}$ and V1G1 are mutually exclusive. Using purified His–V1G1 bound to Ni–NTA resin we were able to pull down FLAG–$p150^{Glued}$ from lysates of transfected HeLa cells only in the presence of purified GST–RILP (Fig. 1E). These data indicate that RILP can bind to V1G1 and $p150^{Glued}$ at the same time.

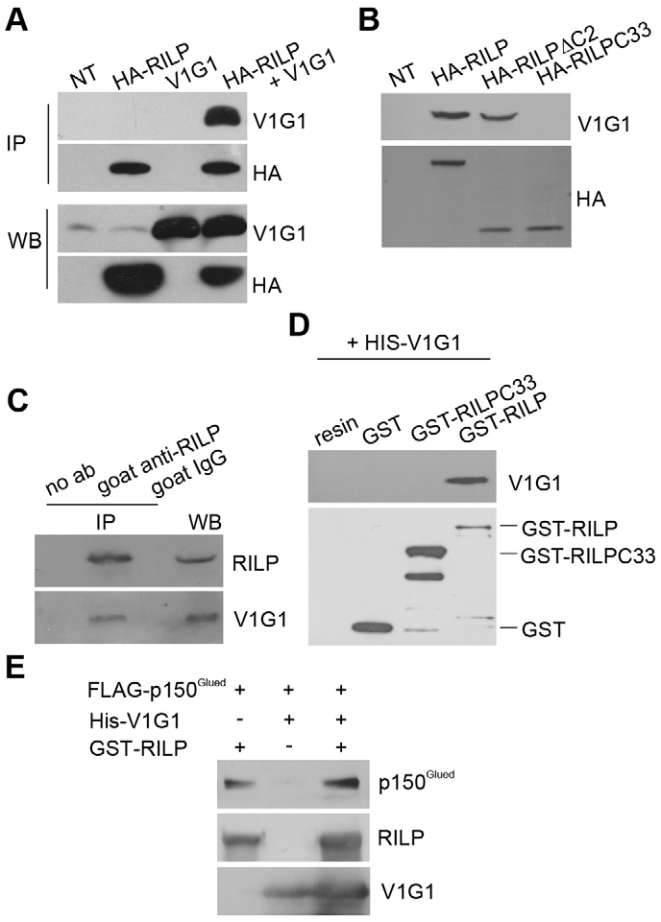

Fig. 1. RILP and V1G1 interact directly. (A) Lysates of control HeLa cells (NT) or cells expressing HA–RILP, V1G1 or both were subjected to immunoprecipitation using an anti-HA antibody. Lysates (WB) and immunoprecipitates (IP) were subjected to western blot analysis using anti-HA and anti-V1G1 antibodies. (B) Immunoprecipitates obtained using anti-HA antibodies from control HeLa cells or cells expressing V1G1 and HA–RILP, HA–RILPΔC2 or HA–RILPC33 were subjected to western blot analysis using anti-HA or anti-V1G1 antibodies. (C) Total extracts of HeLa cells (WB) and immunoprecipitates obtained with no antibodies (no ab), with goat anti-RILP or with goat IgG, as indicated, were subjected to western blot analysis using chicken anti-V1G1 and rabbit anti-RILP antibodies. (D) Glutathione resin alone or bound to purified GST, GST–RILPC33 or GST–RILP was incubated with purified His-tagged V1G1. After affinity chromatography, proteins were subjected to western blot analysis using anti-GST and anti-V1G1 antibodies. (E) Bacterially expressed and purified His-tagged V1G1 was incubated with total extract of HeLa cells expressing FLAG–$p150^{Glued}$ in the presence or absence of purified GST–RILP and pulled-down using Ni–NTA resin. As a positive control, GST–RILP was pulled down after incubation with total extract of HeLa cells expressing FLAG–$p150^{Glued}$. Proteins were then loaded onto SDS-PAGE gels and subjected to western blot analysis using anti-$p150^{Glued}$, anti-V1G1 and anti-GST antibodies.

Journal of Cell Science (2014) 127, 2697–2708 doi:10.1242/jcs.142604

RILP expression levels affect V1G1 abundance

To investigate the role of this interaction, we decided to analyze whether modulation of RILP expression levels affected V1G1 abundance. Interestingly, upon RILP overexpression, the total amount of the V1G1 subunit in HeLa cells was reduced (Fig. 2A). By contrast, in RILP-silenced cells, the amount of V1G1 was strongly increased (Fig. 2B). Importantly, RILP overexpression or silencing did not affect V1C1 and V0D1, two other V-ATPase subunits (Fig. 2A,B), indicating that RILP regulates V1G1 specifically. Notably, expression of RILPΔC2 or RILPC33 did not affect V1G1 abundance (Fig. 2C), suggesting that only the entire protein is able to act on V1G1 protein abundance.

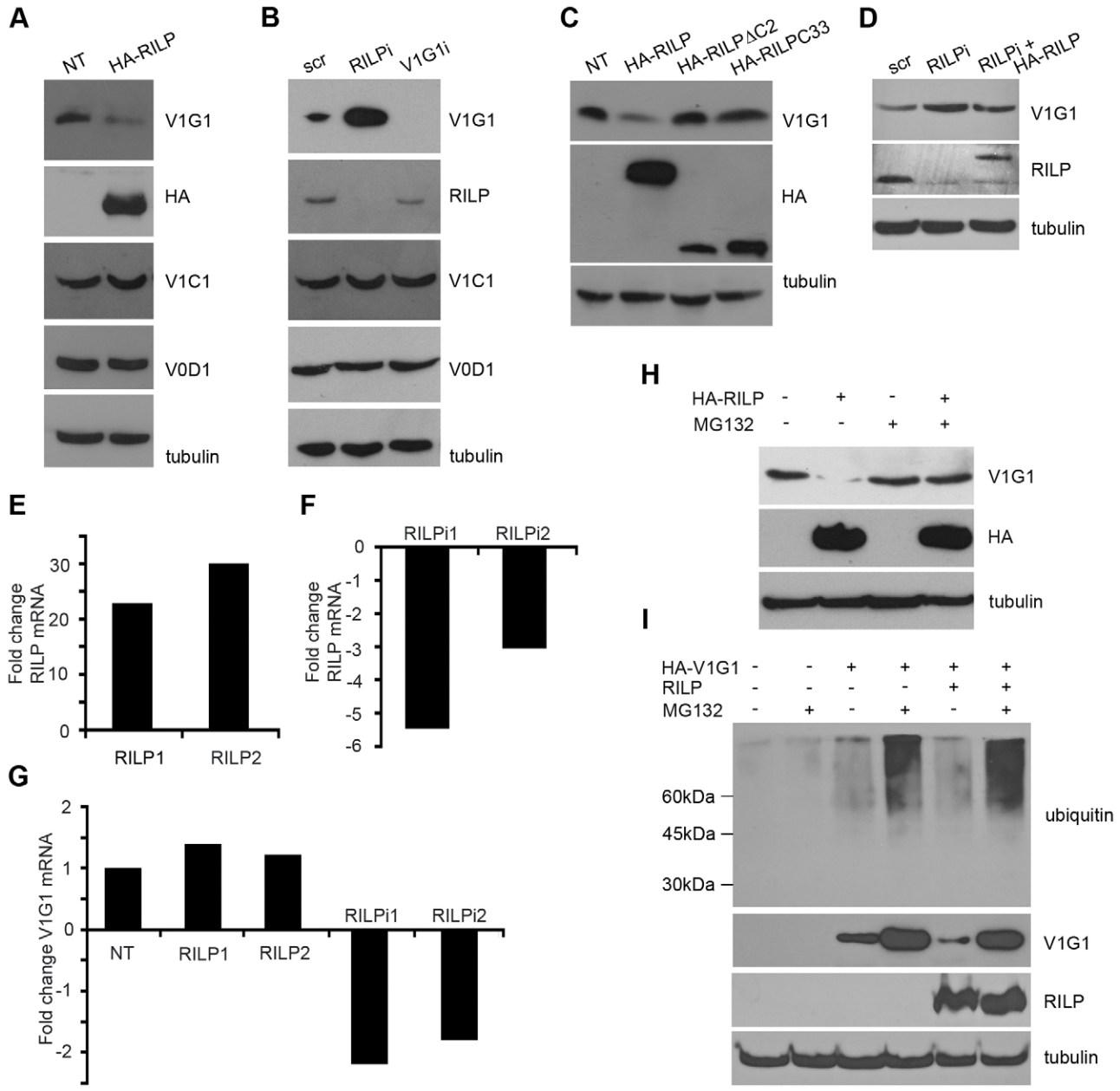

Fig. 2. RILP modulates V1G1 abundance in HeLa cells through ubiquitylation-dependent proteasomal degradation. (A) Lysates of control HeLa cells (NT) or cells expressing HA–RILP were subjected to western blot analysis using primary antibodies against V1G1, HA, V1C1, V0D1 and tubulin. (B) Cells treated with control siRNA (scr), RILP-specific siRNA (RILPi) or V1G1-specific siRNA (V1G1i) were subjected to western blot analysis using primary antibodies against V1G1, RILP, V1C1, V0D1 and tubulin. (C) Lysates of control HeLa cells or cells expressing HA–RILP, HA–RILPΔC2 or HA–RILPC33 were subjected to western blot analysis using anti-V1G1, anti-HA and anti-tubulin antibodies. (D) Cells treated with control siRNA or RILP-specific siRNA and transfected with HA–RILP, as indicated, were subjected to western blot analysis using anti-V1G1, anti-RILP and anti-tubulin antibodies. (E–G) Real-time PCR was performed on control HeLa cells, or cells expressing HA–RILP (RILP1 and RILP2) or silenced for RILP (RILPi1 and RILPi2), and the amount of RILP (E,F) or of V1G1 (G) was quantified relative to the control GAPDH RNA transcript. (H) Control cells or cells expressing HA–RILP, as indicated, were either untreated or treated with the proteasomal inhibitor MG132. Lysates were then subjected to western blot analysis with antibodies against V1G1, HA and tubulin. (I) Control cells or cells transfected with HA–V1G1 and RILP, as indicated, were either untreated or treated with MG132. Lysates were subjected to western blot analysis using antibodies against RILP, V1G1 and tubulin, and to immunoprecipitation using an anti-HA antibody. Immunoprecipitates were subjected to western blot analysis using an anti-ubiquitin antibody.

Journal of Cell Science (2014) 127, 2697–2708 doi:10.1242/jcs.142604

Furthermore, overexpression of HA-tagged RILP was able to partially rescue the effect on V1G1 abundance in RILP-silenced cells, thus excluding off-target effects (Fig. 2D).

To establish whether the observed changes in the amount of V1G1 protein were a consequence of mRNA abundance, we checked V1G1 mRNA expression using real-time PCR (Fig. 2G). As expected, in cells transfected with HA–RILP, RILP mRNA was increased, whereas in RILP-silenced cells, RILP mRNA levels decreased (Fig. 2E,F). Interestingly, we found that the amount of V1G1 mRNA upon RILP overexpression was slightly increased, whereas it was decreased upon RILP silencing (Fig. 2G). Thus, mRNA expression seems to be altered in order to counteract the effects on the amount of V1G1 protein that are caused by RILP overexpression or silencing.

RILP induces proteasomal degradation of V1G1

As we established that RILP expression levels regulate the amount of V1G1, we then decided to investigate whether RILP was responsible for the proteasomal degradation of V1G1. We overexpressed RILP and treated cells with the proteasome inhibitor MG132. Under these conditions, the endogenous V1G1 protein level did not decrease, suggesting that RILP regulates the proteasomal degradation of V1G1 (Fig. 2H). We then decided to investigate whether V1G1 was ubiquitylated. We expressed HA–V1G1 in HeLa cells in the presence or absence of the proteasomal inhibitor MG132 and in the presence or absence of RILP overexpression. Lysates of cells were then immunoprecipitated with anti-HA resin and subjected to western blot analysis using an anti-ubiquitin antibody. Ubiquitylation of V1G1 was present in all samples where HA–V1G1 was expressed and immunoprecipitated, but was increased in the presence of MG132, suggesting a strong regulation of V1G1 mediated by the proteasome. The amount of V1G1 protein decreased upon RILP overexpression, whereas treatment with MG132 partially rescued V1G1 levels and strongly increased the level of ubiquitylated forms of V1G1. Hence, taking into consideration V1G1 levels, RILP overexpression induces V1G1 ubiquitylation (Fig. 2I).

RILP recruits V1G1 to late endosomal and/or lysosomal membranes

We next analyzed whether RILP is responsible for the recruitment of V1G1 to membranes. We treated cells with MG132 in order to prevent V1G1 ubiquitin-dependent proteasomal degradation induced by RILP, and we looked at the cytosolic and membrane distribution of endogenous V1G1 in control cells and in cells overexpressing RILP. As loading controls, we used GAPDH, a cytosolic protein, and V0D1, a membrane subunit of V-ATPase. Expression of HA–RILP did not change the membrane or cytosol distribution of GAPDH and V0D1. The analysis of the distribution of V1G1 showed that the amount of membrane-associated V1G1 increased upon RILP overexpression, whereas the amount of cytosolic V1G1 decreased (Fig. 3A). Indeed, RILP overexpression increased membrane localization of V1G1 by about 30%, whereas cytosolic V1G1 was reduced by 85% compared with control (Fig. 3B). These data demonstrate that V1G1 membrane localization increases upon RILP overexpression, and they suggest that RILP could recruit V1G1 to endosomal and/or lysosomal membranes.

Having shown that RILP controls the amount of V1G1 and its recruitment to membranes, we decided to investigate whether V1G1 binds to RILP when it is in complex with other V-ATPase subunits. We used an anti-HA resin to immunoprecipitate HA-tagged RILP from lysates of HeLa cells expressing HA-tagged

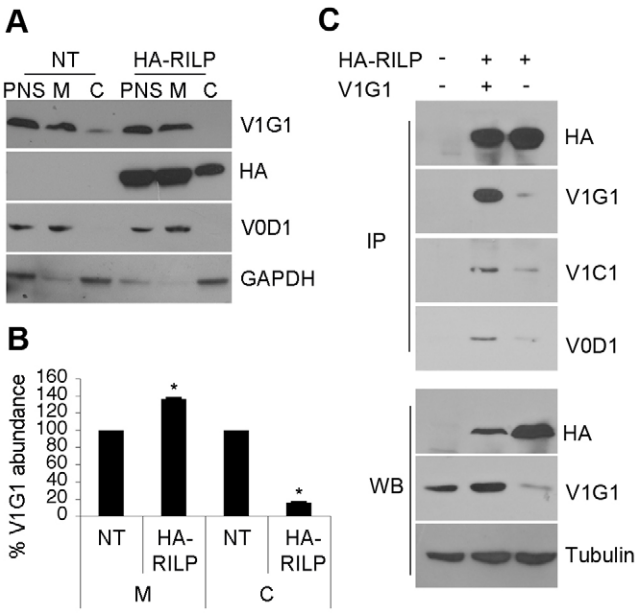

Fig. 3. RILP recruits V1G1 to late endosomal and/or lysosomal membranes. (A) Post-nuclear supernatants (PNS), cytosol (C) and membrane (M) fractions of control (NT) HeLa cells or cells expressing HA–RILP, as indicated, treated with MG132 at 3 h before harvesting, were subjected to western blot analysis using antibodies against V1G1, HA, V0D1 and GAPDH. (B) Quantification of the amount of V1G1 protein present in membrane and cytosol fractions, normalized to V0D1 and GAPDH, respectively. Data represent the mean±s.e.m. (three independent experiments); $*P<0.05$. (C) Lysates of control HeLa cells or cells expressing HA–RILP and V1G1 or just HA–RILP were subjected to immunoprecipitation using mouse anti-HA antibody. Lysates (WB) and immunoprecipitates (IP) were subjected to western blot analysis using antibodies against HA, V1G1, V1C1, V0D1 or tubulin.

RILP and endogenous or overexpressed V1G1. In both immunoprecipitates, we observed the presence not only of V1G1 but also of V1C1 and V0D1, two other V-ATPase subunits (Fig. 3C). Larger amounts of co-immunoprecipitated V1G1, obtained when V1G1 was overexpressed, led to increased co-immunoprecipitation of the other two subunits (Fig. 3C). These data suggest that V1G1 interacts with RILP alone or complexed with the other subunits, thus suggesting that RILP could be important for controlling the assembly of the entire pump at the endosomal membranes by recruiting V1G1.

We also used confocal immunofluorescence to analyze the intracellular localization of V1G1 upon RILP overexpression. As commercially available antibodies against the V1G1 subunit of V-ATPase do not work in immunofluorescence, we looked at the localization of the overexpressed HA-tagged V1G1 subunit. As expected, V1G1 was partially colocalized with Lamp1 on late endosomal and lysosomal structures (Fig. 4). Expression of RILP caused clustering of late endosomal and lysosomal structures, as reported previously (Cantalupo et al., 2001; Colucci et al., 2005b), and HA-tagged V1G1 was localized on the clustered structures that were generated and marked by GFP–RILP (Fig. 4A). Interestingly, upon RILP overexpression, the colocalization percentage of V1G1 with Lamp1 is increased (Fig. 4A,B). By contrast, expression of RILP-C33, the deletion mutant containing only the C-terminal half of RILP that does not interact with V1G1, decreased colocalization with Lamp1 (Fig. 4A,B). These data suggest that the localization of V1G1

Journal of Cell Science (2014) 127, 2697–2708 doi:10.1242/jcs.142604

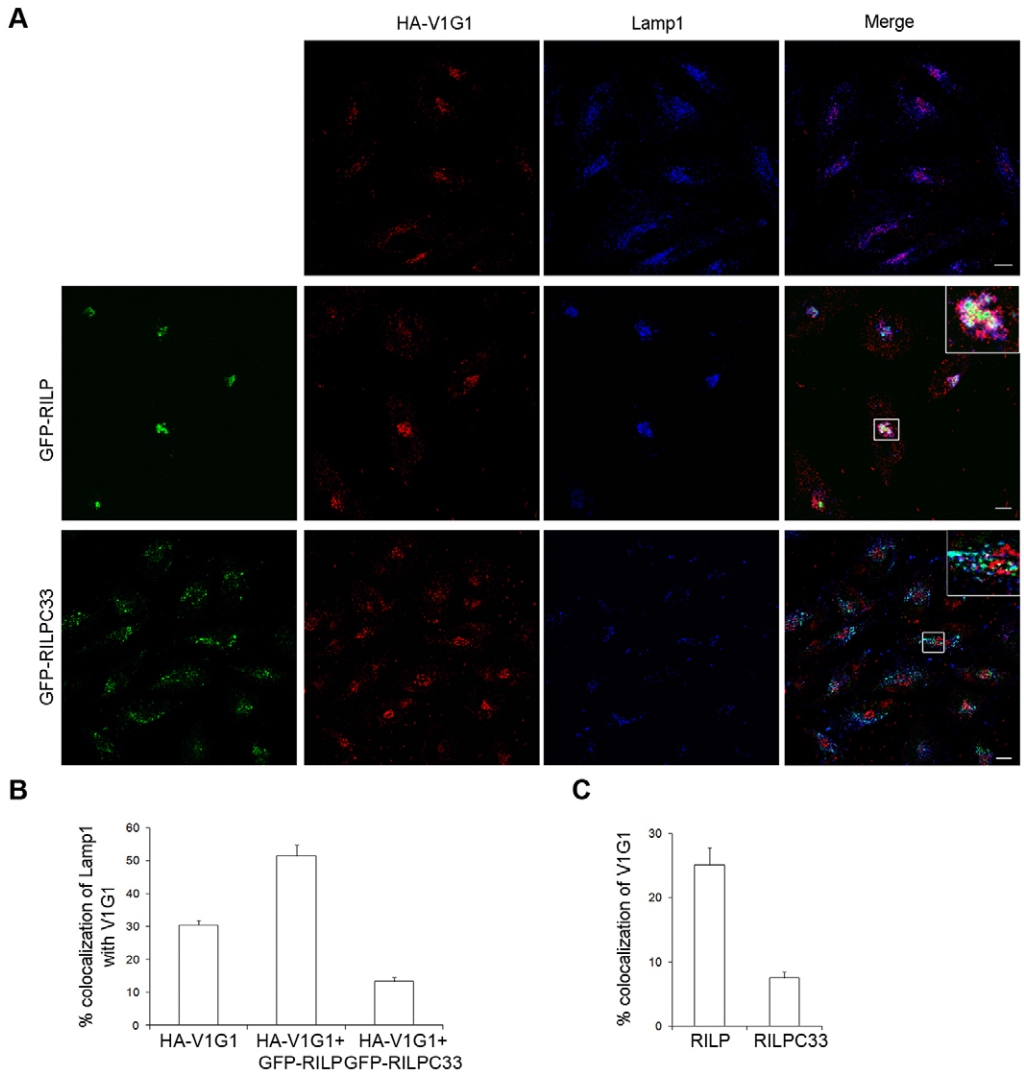

Fig. 4. RILP partially colocalizes with V1G1 on late endosomal and lysosomal organelles. (A) HeLa cells transfected with HA–V1G1 (upper panels), co-transfected with GFP–RILP and HA–V1G1 (middle panels) or co-transfected with GFP–RILPC33 and HA–V1G1 (lower panels) were fixed and immunostained for Lamp1 and HA. Insets show enlargements of the indicated areas. Scale bars:10 μm. (B) Quantification of the colocalization between Lamp1 and V1G1. (C) Quantification of the colocalization of V1G1 with GFP–RILP or GFP–RILPC33. Data represent the mean±s.e.m. (three independent experiments, ≥50 cells per experiment).

on late endosomal and/or lysosomal membranes is regulated by RILP. Furthermore HA-tagged V1G1 partially colocalized with RILP on late endosomal and/or lysosomal structures labelled with Lamp1, whereas very little colocalization was detected with RILPC33 (Fig. 4A). Quantification of the immunofluorescence data (Fig. 4C) indicates that <10% of HA–V1G1 colocalized with RILPC33, thus confirming the interaction data.

In addition, we analyzed the effects of RILP silencing on the localization of HA-tagged V1G1 (Fig. 5). Interestingly, in RILP-depleted cells (RILPi) the colocalization of HA-tagged V1G1 with Lamp1 decreased, thus confirming the role of RILP in recruiting V1G1 to late endosomal and lysosomal membranes (Fig. 5). In addition, upon RILP silencing, the colocalization of HA-tagged V1G1 with giantin (also known as GOLGB1), a marker of the Golgi complex, strongly increased, indicating that, in the absence of RILP, V1G1 localizes mainly to other compartments (Fig. 5). Taken together, these data indicate that RILP recruits V1G1 to late endosomal and lysosomal membranes and suggest that RILP could be important for the assembly of the pump on these organelles.

RILP is in complex with V1G1 together with Rab7

RILP is a Rab7 effector protein and, thus, in order to investigate whether Rab7 is also involved in the regulation of V1G1, we transiently overexpressed or silenced Rab7 and looked at V1G1 abundance (Fig. 6A,B). Interestingly, Rab7 overexpression did not affect V1G1 abundance, whereas Rab7 silencing caused a strong decrease in the amount of V1G1 (Fig. 6A,B). Furthermore, the decrease in the amount of V1G1 caused by RILP overexpression was counteracted by Rab7 overexpression (Fig. 6C), thus suggesting that when RILP binds to Rab7 it does not induce V1G1 degradation.

In order to further investigate the role of Rab7 in the interaction between RILP and V1G1, we used HeLa cells to co-express HA–RILP, HA–RILPΔC2, HA–RILPC33, Myc–Rab7 and V1G1 in different combinations, and we immunoprecipitated V1G1 using a specific anti-V1G1 antibody (Fig. 6D). Immunoprecipitates were then analyzed for the presence of the different recombinant proteins. As expected, V1G1 was able to co-immunoprecipitate HA–RILP and HA–RILPΔC2 but not HA–RILPC33 (Fig. 6D, lanes 2–4). Interestingly, V1G1 was also able to co-immunoprecipitate Rab7 (Fig. 6D, lane 5), although in the two-hybrid system we did not detect interaction between these two proteins (supplementary material Fig. S1). However, co-immunoprecipitation of V1G1 and Rab7 was seen both upon exogenous HA–RILP expression (Fig. 6D, lane 7) and in the presence of endogenous RILP (Fig. 6D, lane 5). In RILP-silenced cells, Rab7 no longer co-immunoprecipitated with V1G1 (Fig. 6D,

Journal of Cell Science (2014) 127, 2697–2708 doi:10.1242/jcs.142604

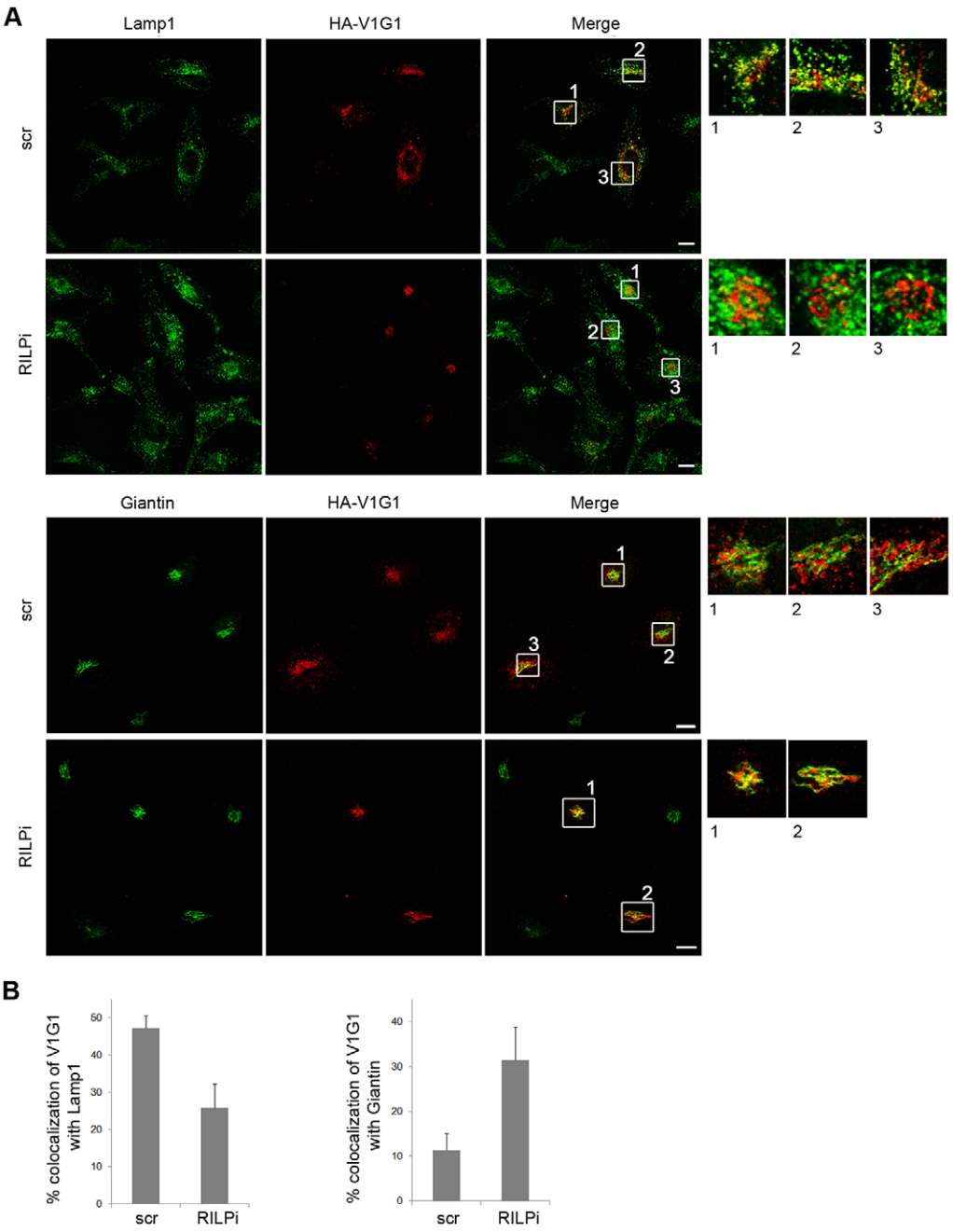

Fig. 5. RILP depletion affects V1G1 intracellular localization. (A) Control (scr) and RILP-depleted cells (RILPi) were transfected with HA–V1G1, fixed and immunostained for Lamp1, HA and giantin. Enlargements shown on the right correspond to the numbered squares in the merged images. Scale bars:10 μm. (B) Quantification of the colocalization between V1G1 and Lamp1 or V1G1 and giantin. Data represent the mean±s.d. (three independent experiments, ≥50 cells per experiment).

lane 6). These data indicate that V1G1 does not interact directly with Rab7 and that RILP is able to interact simultaneously with Rab7 and V1G1. Indeed, expression of the RILP truncated forms RILPΔC2 or RILPC33, which bind to and sequester V1G1 and Rab7, respectively, abolished the co-immunoprecipitation of Rab7 (Fig. 6D, lanes 12–13). Taken together, these data indicate that Rab7 recruits RILP to endolysosomal membranes, and RILP in turn recruits V1G1, whereas RILP induces V1G1 proteasomal degradation when it is not bound to Rab7.

V-ATPase activity is regulated by RILP

RILP is required for the biogenesis of MVBs and, together with Rab7, it regulates late endocytic traffic (Progida et al., 2007). Acidification, triggered by V-ATPase, is required for the formation of MVBs (Aniento et al., 1996; Clague et al., 1994; Marshansky and Futai, 2008; Trajkovic et al., 2008). Thus, RILP might coordinate the biogenesis of MVBs through V-ATPase activity regulation, by controlling the amount and localization of V1G1. In order to investigate whether RILP influences V-ATPase activity, we used LysoTracker Red, a marker of acidic compartments that stains vesicles with an internal pH of <6.5, in HeLa cells depleted of RILP (RILPi) (Fig. 7A). The samples were analyzed by live microscopy, and LysoTracker Red intensity in RILPi samples relative to controls (scr) was quantified (Fig. 7B). Interestingly, the levels of LysoTracker Red intensity were increased more than twofold in RILPi cells, suggesting a role for RILP in controlling V-ATPase activity (Fig. 7A,B). Furthermore, the distribution of acidic compartments was more diffuse and peripheral in RILP-depleted cells compared with control cells.

Journal of Cell Science (2014) 127, 2697–2708 doi:10.1242/jcs.142604

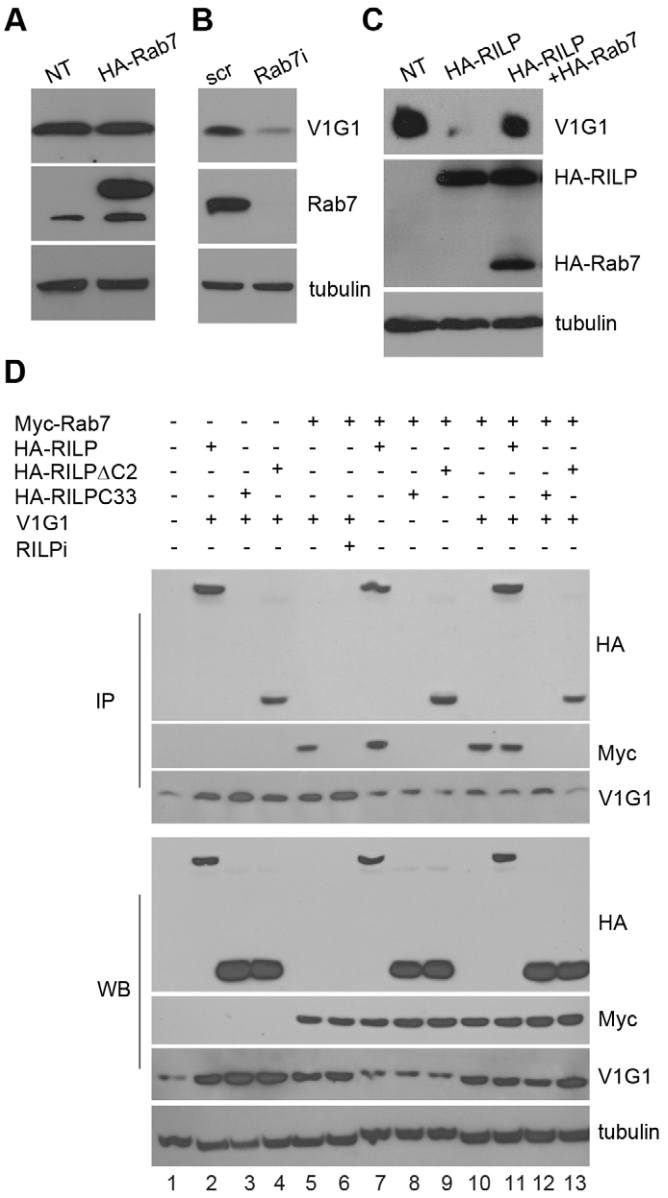

Fig. 6. Role of Rab7 in the regulation of V1G1. Lysates of control HeLa cells (NT) or cells expressing HA–Rab7 (A) or of HeLa cells treated with control siRNA (scr) or Rab7-specific siRNA (Rab7i) (B) were subjected to western blot analysis using anti-V1G1, anti-Rab7 and anti-tubulin antibodies. (C) HeLa cells transfected with HA–RILP and HA–Rab7, as indicated, were subjected to western blot analysis using anti-V1G1, anti-HA and anti-tubulin antibodies. (D) Whole-cell lysates (WB) of HeLa cells expressing Myc–Rab7, HA–RILP, HA–RILPΔC2, HA–RILPC33 and/or V1G1, as indicated, were immunoprecipitated using mouse anti-V1G1 antibodies. In one sample, RILP was also silenced (RILPi) before expression of Myc–Rab7 and V1G1 (lane 6). Immunoprecipitates (IP) were subjected to western blot analysis using rabbit anti-Myc, rabbit anti-HA and chicken anti-V1G1 antibodies.

V1G1 is fundamental for V-ATPase activity

Because we had demonstrated that RILP is important for acidification and controls V1G1 abundance and recruitment to late endosomal and lysosomal membranes, we decided to investigate the relevance of V1G1 to V-ATPase activity. In order to monitor how variations of V1G1 abundance affect V-ATPase activity, we monitored cathepsin D maturation in HeLa cells that overexpressed V1G1 or that were silenced for V1G1 either transiently or stably. Cathepsin D is synthesized as preprocathepsin D precursor, which is converted into procathepsin D (52 kDa) in the endoplasmic reticulum, and then undergoes further proteolytic processing in the acidic milieu of late endosomes and lysosomes, being converted in a 44-kDa form and finally into the 32-kDa mature form. Lysates of control HeLa cells and of V1G1-silenced or V1G1-overexpressing cells were subjected to western blot analysis with an anti-cathepsin-D antibody that recognized the 52-kDa, 44-kDa and 32-kDa forms (Fig. 7C). In control cells, the 52-kDa and the 44-kDa forms represented <30% of the total cathepsin D staining, whereas, as expected, treatment with bafilomycin A1, a high-affinity inhibitor of V-ATPase, caused the accumulation of the immature forms and reduced the amount of the mature 32-kDa form to <5% (Fig. 7C,D). Transient or stable overexpression (in two independent clones) of V1G1 caused a strong increase in the amount of immature cathepsin D forms, whereas the mature 32-kDa form represented <25% of the total cathepsin D staining (Fig. 7C,D). Similarly, transient or stable depletion of V1G1 (in two independent clones) caused an accumulation of the immature forms, whereas the mature 32-kDa form of cathepsin D accounted for <25% of the total cathepsin D staining (Fig. 7C,D). By contrast, no changes were detected in cells transfected with a construct expressing a control short-hairpin (sh)RNA (Fig. 7C,D).

As V1G1 seems to be important to ensure proper V-ATPase activity, we wanted to investigate the effect on late endosomes and lysosomes when cells were depleted of V1G1. We therefore used two different markers of acidic compartments – LysoTracker Red, which accumulates in acidic compartments, and LysoSensor DND-192, which labels less acidic compartments than LysoTracker Red – and we allowed HeLa cells that were stably depleted of V1G1 (in two independent clones) to internalize fluorescently labeled transferrin. Afterwards, we quantified the relative amount of transferrin that colocalized with LysoTracker-Red- or LysoSensor-positive endosomes, by using confocal microscopy analysis (supplementary material Fig. S2). Internalized transferrin mainly localizes to sorting and recycling early endosomes, and only a small percentage of it reaches late endosomes and lysosomes to be degraded (Dautry-Varsat et al., 1983; Hopkins and Trowbridge, 1983). Changes in the percentage of transferrin colocalizing with endocytic degradative compartments represent a clear alteration of the endocytic route (Roxrud et al., 2009).

The levels of transferrin in LysoTracker-positive structures increased in both clones depleted of V1G1, and the increase was stronger in LysoSensor-positive endosomes (supplementary material Fig. S2). These results confirm the importance of V1G1 for the V-ATPase activity, as the depletion of this subunit causes accumulation of transferrin in acidic compartments, suggesting impaired degradation, and thus malfunctioning of late endosomes and lysosomes. Taken together, these data demonstrate that changes in the amount of V1G1 impair V-ATPase activity.

DISCUSSION

V-ATPases are highly conserved enzymes that couple ATP hydrolysis to proton transport across membranes, and they consist of two domains and multiple subunits and are localized to the membrane of several organelles (Cipriano et al., 2008; Toei et al., 2010). The G subunit of the V-ATPase V1 domain is part, together with the E subunit, of the peripheral stator stalks

Journal of Cell Science (2014) 127, 2697–2708 doi:10.1242/jcs.142604

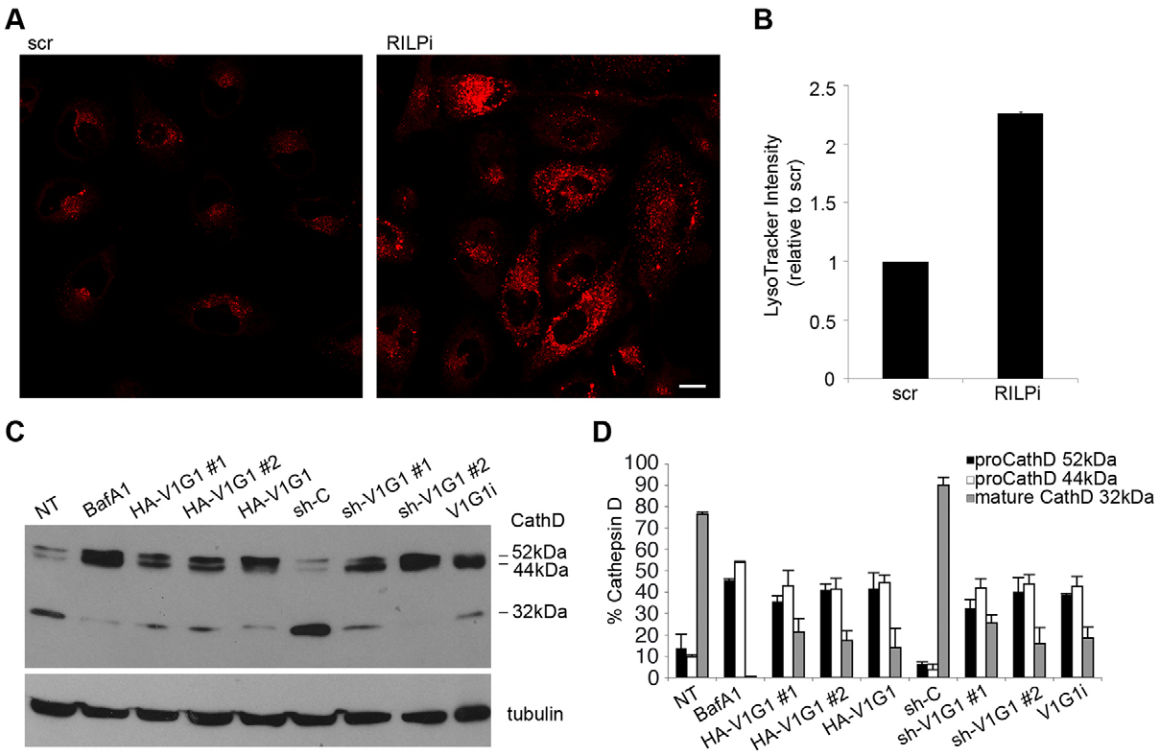

Fig. 7. RILP and V1G1 control V-ATPase activity. (A) HeLa cells treated with control RNA (scr) or RILP-specific siRNA (RILPi) were incubated with LysoTracker Red for 30 min and analyzed by live microscopy. Scale bar: 10 μm. (B) The LysoTracker Red intensity, relative to that of scr, was quantified. Data represent the mean±s.d. (three independent experiments, ≥50 cells per experiment). (C) Lysates of control HeLa cells (NT), cells treated with bafilomycin A1, cells transiently or stably expressing (clones 1 and 2) HA–V1G1 or transiently or stably expressing (clones 1 and 2) sh-V1G1 or control RNA (sh-C) were subjected to western blot analysis using anti-cathepsin-D and anti-tubulin antibodies. (D) Quantification of cathepsin D forms. Data represent the mean±s.e.m. (three independent experiments).

responsible for structurally and functionally linking the peripheral V1 sector to the membrane V0 sector of the pump (Armbrüster et al., 2003; Ohira et al., 2006). There are two isoforms of the G subunit – G1 is ubiquitously expressed, whereas G2 is specifically expressed in central nervous system neurons (Murata et al., 2002). Here, we have identified the G1 subunit of V-ATPase as an RILP-interacting protein. We have proved that the interaction is physiological, as it was detected by co-immunoprecipitation of overexpressed (Fig. 1A) but also endogenous proteins (Fig. 1C). Furthermore, we have proved that the interaction is direct, as it was also detectable between bacterially expressed and purified proteins (Fig. 1D). In addition, our data indicate that V1G1 interacts with the N-terminal half of RILP (Figs 1,6D; supplementary material Fig. S1), in contrast to Rab7, which binds in the C-terminal half of RILP (Cantalupo et al., 2001). Interestingly, the RILP–V1G1 complex can interact with the dynactin projecting arm $p150^{Glued}$ (Fig. 1E), suggesting that RILP could simultaneously control endosome acidification and translocation towards the microtubule organizing center.

What is the functional meaning of this interaction?

Our data indicate that RILP regulates the recruitment of V1G1 to endosomes and lysosomes. Overexpression of RILP increases the colocalization of V1G1 with the late endosomal and lysosomal marker Lamp1, whereas expression of the RILPC33 mutant, which is unable to bind to V1G1, decreases it (Fig. 4). In addition, overexpression of RILP increases the amount of V1G1 present in membranes and drastically decreases V1G1 in the cytosol (Fig. 3A,B). In agreement, in RILP-silenced cells colocalization of V1G1 with Lamp1 decreases, whereas co-localization with giantin increases (Fig. 5), indicating that RILP is important for the recruitment of V1G1 to late endosomal and lysosomal membranes. Thus, GTP-bound Rab7 recruits RILP to late endosomes and lysosomes (Cantalupo et al., 2001), and RILP, in turn, recruits V1G1 to these organelles. In fact, we demonstrated by co-immunoprecipitation that RILP is able to bind simultaneously to V1G1 at its N-terminal half and Rab7 at its C-terminal half (Fig. 6D). Also, we established that V1G1 is not able to bind to Rab7 directly, because V1G1 is not able to interact with Rab7 in the two-hybrid system (supplementary material Fig. S1), and it is not able to co-immunoprecipitate Rab7 in the absence of RILP (Fig. 6D).

As V1G1 is important for V-ATPase assembly and function (Ohira et al., 2006; Tomashek et al., 1997), the recruitment of V1G1 to endosomal or lysosomal membranes is likely to contribute to the correct assembly and, consequently, functioning of the pump. In fact, our data show that V1G1, when binding to RILP, can also be in complex with other subunits of the cytosolic and membrane domain of V-ATPase (Fig. 3C), thus suggesting that RILP could control not only the recruitment of V1G1 to endosomal and lysosomal membranes but also the assembly of the entire pump. Furthermore, we have demonstrated that RILP modulates the activity of the pump on late endosomes and lysosomes, controlling V1G1 localization (Figs 4,5). Indeed, in RILP-depleted cells we detected mislocalization of V1G1 to other organelles (Fig. 5) and a different intracellular distribution and higher

Journal of Cell Science (2014) 127, 2697–2708 doi:10.1242/jcs.142604

intensity of LysoTracker Red (Fig. 7A,B). These data, together with the previously reported inhibition of EGFR degradation and increase in Lamp levels upon RILP silencing (Progida et al., 2006; Progida et al., 2007), suggest that there is a block of endosomal maturation caused by the failed recruitment of the proton pump to Rab7-labeled endosomes.

We have shown previously that RILP is important for the formation of MVBs (Progida et al., 2007; Progida et al., 2006). As MVB formation is dependent on the luminal acidic pH of endosomes and thus on the acidification triggered by V-ATPase (Aniento et al., 1996; Clague et al., 1994; Marshansky and Futai, 2008; Trajkovic et al., 2008), our data support the idea that RILP might coordinate the biogenesis of MVBs through regulation of V1G1 activity.

Our data also demonstrate that RILP regulates V1G1 subunit abundance. Overexpression of RILP causes a reduction in the amount of V1G1, whereas, in RILP-silenced cells, the amount of V1G1 is strongly increased (Fig. 2A,B). Furthermore, we established that RILP induces V1G1 ubiquitylation-dependent proteasomal degradation (Fig. 2I). Thus, RILP promotes the recruitment of V1G1 to endosomal membranes but also induces V1G1 degradation. How are these two different and contrasting functions regulated? Our data indicate that overexpression of Rab7 has no effect on V1G1 abundance, whereas Rab7 silencing causes a strong decrease in the amount of V1G1 (Fig. 6A,B). Hence, these data suggest that when RILP is bound to Rab7 it recruits V1G1 to membranes, whereas an excess of RILP that is not bound to Rab7 (as in the case of RILP overexpression or Rab7 silencing) leads to V1G1 degradation. Therefore, the amount of V1G1 is strictly regulated by the availability of cytosolic RILP.

Previously, we have observed that expression of the Rab7T22N mutant, which is unable to recruit RILP to late endosomal or lysosomal membranes, causes a strong decrease in LysoTracker Red staining (Bucci et al., 2000), thus indicating an increase in pH of intracellular organelles, possibly caused by impaired V-ATPase assembly and function due to the lack of RILP-mediated recruitment of V1G1. These data seem to contrast with the fact that RILP silencing causes an increase in LysoTracker intensity (Fig. 7A,B). However, in cells expressing the Rab7T22N mutant, RILP is still present but it cannot be recruited to endosomes and could, instead, induce V1G1 degradation.

We also demonstrated that a proper amount of V1G1 seems to be fundamental for the correct functioning of the pump. Overexpression or silencing of the V1G1 subunit causes a strong inhibition of cathepsin D maturation, similar to what happens when treating the cells with bafilomycin A1, an inhibitor of the vacuolar pump (Fig. 7C,D). Moreover, V1G1 silencing causes the accumulation of transferrin in acidic compartments, suggesting that it is linked to malfunctioning of late endosomes and lysosomes (supplementary material Fig. S2). These data are in agreement with previously published data suggesting that changes in V1G1 expression destabilize the E subunit, influencing V-ATPase assembly (Ohira et al., 2006; Tomashek et al., 1997). The V1G1 subunit thus seems to be a crucial subunit not only for correct assembly of the vacuolar pump but also for V-ATPase function, as changes in the amount of V1G1 have strong negative effects on processes regulated by V-ATPase.

The discovery of the interaction between RILP and V1G1 is of importance, as it reveals a new mechanism of regulation of the V-ATPase, mediated by RILP. In particular, our data demonstrate that RILP regulates V1G1 abundance and is crucial for the regulation of V-ATPase at the level of late endosomes and lysosomes, promoting assembly and activation of the proton pump on these organelles (Fig. 8).

V-ATPase has been proposed as a drug target for several diseases and processes (Hinton et al., 2009; Kartner and Manolson, 2012). Plasma membrane V-ATPases are important for sperm maturation and viability (Pietrement et al., 2006), for acid secretion by certain kinds of renal cells (the malfunctioning

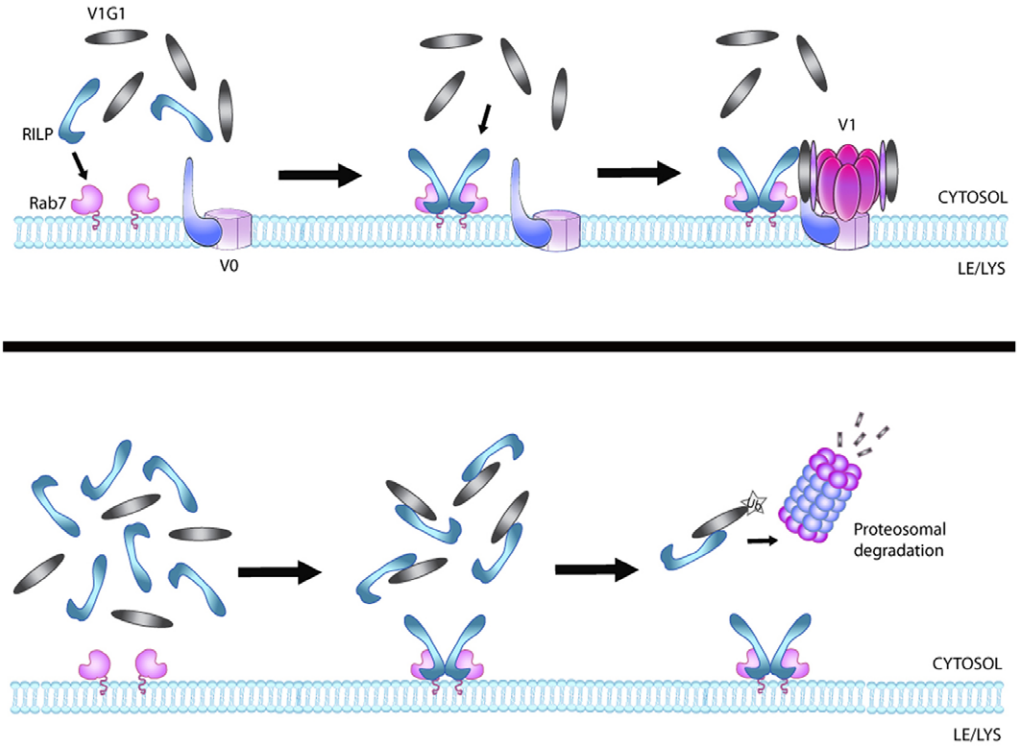

Fig. 8. Proposed model for the functional interactions between RILP, V1G1 and Rab7. RILP strictly regulates V1G1 abundance and localization, promoting activation of the proton pump on late endosomes (LE) and lysosomes (LYS). Upper panel, the binding of RILP to Rab7 induces V1G1 recruitment to late endosomal and lysosomal membranes and, in turn, promotes assembly of the pump on these membranes. Lower panel, the ratio of RILP to Rab7 is fundamental for V1G1 protein abundance; an excess of RILP that is not bound to Rab7 (as is the case during RILP overexpression or Rab7 silencing) leads to V1G1 ubiquitylation and degradation through a proteasome-dependent mechanism.

Journal of Cell Science (2014) 127, 2697–2708 doi:10.1242/jcs.142604

of which causes renal tubular acidosis) (Karet et al., 1999; Smith et al., 2000) and for osteoclast bone degradation (Frattini et al., 2000; Toyomura et al., 2003), which, if altered, causes osteopetrosis and osteoporosis. Importantly, in many tumor cell lines, V-ATPases are abundant in plasma membranes, and their activity in plasma membranes has been directly correlated with invasiveness (Sennoune et al., 2004a; Sennoune et al., 2004b; Sennoune and Martinez-Zaguilan, 2012). The tumor acidic microenvironment plays a key role in tumor development and progression, as it influences resistance to chemotherapy, proliferation and formation of metastases (Hernandez et al., 2012). Thus, in order to fight cancer, the use of V-ATPase inhibitors and/or the regulation of V-ATPase assembly have been proposed to control V-ATPase activity (Kane, 2012; Pérez-Sayáns et al., 2009). Our data suggest that modulation of RILP expression could represent a mechanism to regulate V-ATPase activity. Furthermore, the discovery of a functional link between RILP and V-ATPase opens new possibilities for the cellular role of RILP that will have to be further investigated.

MATERIALS AND METHODS

Cells and reagents

Restriction and modification enzymes were from New England Biolabs (Ipswich, MA), chemicals were from Sigma-Aldrich (St Louis, MO) and tissue culture reagents were from Sigma-Aldrich or Invitrogen (Carlsbad, CA). HeLa cells were grown in DMEM supplemented with 10% FBS, 2 mM glutamine, 100 U/ml penicillin and 10 mg/ml streptomycin, in an incubator at 37℃, under 5% CO_2. HeLa cells were stably transfected with pCDNA3_2xHA_V1G1 plasmid or stably silenced using the sh-RNA V1G1 plasmids (sc-36797-SH, Santa Cruz Biotechnology, Santa Cruz, CA). Stable cell lines were selected by adding G-418 (1 mg/ml, Calbiochem, Darmstadt, Germany) to cells transfected with pCDNA3_2xHA_V1G1 plasmid or by adding puromycin (3 µg/ml, Sigma-Aldrich) to V1G1-silenced cells. Where indicated, MG132 (10 µM, C2211 Sigma-Aldrich) was used for 3–5 h.

Plasmid construction

Most Rab7 and RILP constructs used in this study have been described previously (Cantalupo et al., 2001; Colucci et al., 2005a; Progida et al., 2006; Vitelli et al., 1997). The pCDNA3_2xHA_RILP construct was used to amplify a fragment using the following oligonucleotides; 5′-CTTAGAATTCTAATGGAGCCCAGGAGGGCGGCG-3′ and 5′-ATA-AGAATGCGGCCGCTCACCATTCGGGCTCCTGTCCGTGCTG-3′. The fragment, coding for the N-terminal half of RILP, was then digested with *EcoR*I and *Not*I and cloned into the pCDNA3-2xHA vector to obtain a construct for the expression of an HA-tagged RILPΔC2. The V1G1 ORF was amplified from the two-hybrid pACT2-VIG1 construct using the following oligonucleotides; 5′-CTAAGATCTATGGCTAGTCAGTCTC-AGGGG-3′ and 5′-CGCAAGCTTCTATCCATTTATGCGGTAGTT-3′. The amplified fragment was then digested with *Bgl*II and *Hind*III and cloned into the pEGFP-C1 vector to obtain a construct for the expression of GFP-tagged V1G1. The pCDNA3-V1G1 construct was obtained after cloning the *Bgl*II-*Hind*III fragment from the pEGFP-V1G1 vector into the pCDNA3 vector cut with *BamH*I and *Hind*III. To obtain the HA-tagged V1G1, an *EcoR*V-*Xho*I fragment containing the V1G1 ORF was cloned into the pCDNA3_2xHA plasmid. The pCMV6-AC-GFP-V1G1 (RG203317) vectors were obtained from Origene (Rockville, MD). The pEF-FLAG-p150^{Glued} construct has been described previously (Ohbayashi et al., 2012).

Two-hybrid assay

The construct pGBKT7-RILP was used to screen a human liver cDNA library in the pACT2 vector in AH109 yeast cells (Bartel et al., 1993; Suter et al., 2008). Transformants were plated onto synthetic medium lacking His, Leu and Trp. Colonies were picked 5 days later and then assayed for growth on medium lacking Ade, His, Leu and Trp and for β-galactosidase activity (Bartel et al., 1993). Specificity tests were performed by transforming AH109 yeast cells with the pGBKT7 vector or the pGBKT7-Rab7 construct (as a negative controls) or the pGBKT7-RILP wild-type construct, and with the PGADT7-V1G1 construct. Clones were then assayed for growth on selective medium and for β-galactosidase activity using o-nitrophenyl-β-D-galactoside as a substrate (Bartel et al., 1993).

Transfection and RNA interference

Transfection was performed using Metafectene Pro or Metafectene Easy from Biontex (Martinsried, Germany) following the manufacturer's instructions. After 20 h of transfection, cells were processed for immunofluorescence or biochemical assays. For RNA interference, small-interfering (si)RNAs were purchased from MWG-Biotech (Ebersberg, Germany) or Sigma-Aldrich. We used the following oligonucleotides: siRNA-RILP2 sense, 5′-GAUCAAGGCCAAGAUGU-UATT-3′ and antisense, 5′-UAACAUCUUGGCCUUGAUCTT-3′; control RNA sense, 5′-ACUUCGAGCGUGCAUGGCUTT-3′ and antisense, 5′-AGCCAUGCACGCUCGAAGUTT-3′; siRNA-V1G1 sense, 5′-AGAAG-AAGCUCAGGCUGAATT-3′ and antisense, 5′-UUCTGCCTGAGCUU-CUUCUTT-3′; siRNA-Rab7a sense, 5′-GGAUGACCUCUAGGAAGA-ATT-3′ and antisense, 5′-UUCUUCCUAGAGGUCAUCCTT-3′. RILP and Rab7 siRNAs were efficient in silencing as reported previously (De Luca et al., 2008; Progida et al., 2007; Spinosa et al., 2008). Briefly, HeLa cells were plated 1 day before transfection in tissue culture dishes (6-cm diameter). Cells were transfected with siRNAs using Oligofectamine (Invitrogen) for 72 h, re-plated and left for 48 h before performing further experiments.

Antibodies

Rabbit anti-RILP polyclonal antibodies have been described previously (Cantalupo et al., 2001). Goat polyclonal anti-RILP (1:100, sc-82746), rabbit polyclonal anti-RILP (1:100, sc-98331), mouse monoclonal 9E10 anti-Myc (1:500, sc-40), rabbit polyclonal and mouse monoclonal anti-HA (1:500, sc-805 and sc-7392, respectively), mouse monoclonal anti-V1G1 (1:100, sc-25333), mouse monoclonal anti-V0D1 (1:100, sc-81887), goat polyclonal anti-cathepsin-D (1:500, sc-6486) and rabbit polyclonal anti-GAPDH (1:10000, sc-25778) antibodies were from Santa Cruz Biotechnology. Rabbit polyclonal anti-V1C1 (1:1000, 361–375), rabbit polyclonal anti-Rab7 (1:1000, R4779), mouse monoclonal anti-Rab7 (1:1000, R8779) and mouse monoclonal anti-tubulin (1:3000, clone B512) were from Sigma-Aldrich. Chicken polyclonal anti-V1G1 (1:1000, ab15853) and rabbit polyclonal anti-giantin (1:1000, ab24586) were from Abcam (Cambridge, UK). Goat polyclonal anti-GST (1:2000, 27-4577-01) was from GE Healthcare (Buckinghamshire, UK) and rabbit polyclonal anti-ubiquitin (1:500, Z0458) was from DAKO (Glostrup, Denmark). Mouse monoclonal anti-p150 (1:500, 610474) was from BD Bioscience. Secondary antibodies conjugated to fluorochromes or horseradish peroxidase (HRP) were from Invitrogen or SantaCruz Biotechnology.

Membrane-cytosol separation

For analysis of cytosolic and membrane distribution, pellets of HeLa cells were resuspended in homogenization buffer (8% sucrose in 3 mM imidazole). Cells were passed through a 26-gauge needle and centrifuged at 3800 ***g*** for 5 min at 4℃. The post-nuclear supernatant was centrifuged at 50,000 ***g*** for 2 h at 4℃ and fractionated into the high-speed pellet (membrane) and supernantant (cytosol).

Co-immunoprecipitation, pull-down and direct interaction experiments

For immunoprecipitation, we used anti-HA affinity gel (Ezview Red Anti-HA E6779, Sigma) according to the manufacturer's instructions and as described previously (Cogli et al., 2013b). Co-immunoprecipitation of endogenous proteins in HeLa cells was performed using a crosslink immunprecipitation kit (Pierce, Rockford, IL), following the manufacturer's instructions and as described previously (Cogli et al., 2013a).

For direct interaction experiments, GST, GST-tagged and His-tagged proteins were expressed in bacteria and affinity purified as described previously (Chiariello et al., 1999). Glutathione resin alone or bound to purified GST, GST–RILPC33 or GST–RILP was incubated with purified His-tagged V1G1 in PBS with 2 mM $MgCl_2$ and 0.8 mM GTP for 1 h on a rotating wheel. Subsequently, samples were subjected to GST pull-down using the glutathione resin. Samples were then subjected to SDS-PAGE and western blotting. Pull-down experiments were as described previously (Cogli et al., 2013b). Briefly, purified His–V1G1 was bound to Ni–NTA resin and incubated with lysates of HeLa cells transfected with FLAG–$p150^{Glued}$ in the presence or absence of purified GST–RILP for 2 h at 4℃. In addition, as a control, purified GST–RILP was bound to glutathione resin and incubated with lysates of HeLa cells transfected with FLAG–$p150^{Glued}$ for 2 h at 4℃. After incubation, samples were processed for SDS-PAGE and western blot analysis.

Western blotting

HeLa cells were lysed with RIPA buffer (R0278, Sigma-Aldrich) plus protease inhibitor cocktail (Roche, Mannheim Germany). For ubiquitylation experiments, RIPA buffer was supplemented with 20 mM $Na_4P_2O_7$ pH 7.5, protease inhibitor cocktail (Roche), 50 mM NaF, 2 mM PMSF, 10 mM Na_3VO_4 in HEPES pH 7.5 and 5 µM N-ethylmaleimide. Lysates were loaded onto SDS-PAGE gels, and separated proteins were transferred onto polyvinylidene fluoride (PVDF) membrane from Millipore (Billerica, MA). The membrane was blocked in 5% milk in PBS for 30 min at room temperature, incubated with the appropriate antibody and then with a secondary antibody conjugated to HRP (diluted 1:5000).

For incubation with the antibody against ubiquitin, after transferring, the membrane was subjected to a treatment in denaturing solution (6 M guanidium chloride, 20 mM Tris-HCl pH 7.4, 1 mM PMSF and 5 mM β-mercaptoethanol) for 30 min at 4℃, to make proteins more accessible to the antibody. After extensive washing in TBS-T buffer (25 mM Tris-HCl pH 8.0, 150 mM NaCl and 0.05% Tween) the membrane was blocked in 5% bovine serum albumin (BSA) in TBS (25 mM Tris-HCl pH 8, 150 mM NaCl) for 30 min at room temperature, incubated with the anti-ubiquitin antibody and then with a secondary antibody conjugated to HRP (diluted 1:5000). Bands were visualized by using western blot Luminol Reagent (Santa Cruz) or SuperSignal West Pico (Pierce).

Confocal immunofluorescence microscopy

Cells grown on 11-mm round glass coverslips were permeabilized, fixed and incubated with antibodies as described previously (Bucci et al., 1992). Cells were viewed with a Zeiss LSM 510 confocal microscope. In some experiments, cells were incubated with LysoTracker Red or LysoSensor DND-192 (Invitrogen) and Alexa-Fluor-647- or Alexa-Fluor-555-labelled transferrin (Invitrogen) for 30 min. Cells were imaged by live microscopy, and the relative level of transferrin colocalizing with LysoTracker or LysoSensor was quantified.

Standard RNA procedures and quantitative real-time PCR

Total RNA was extracted from HeLa cells by using the RNeasy mini kit according to the manufacturer's instructions (Qiagen, Hilden, Germany). The RNA retrotranscription protocol was performed as described previously (Progida et al., 2010). Quantitative real-time PCR was performed using SYBR Green JumpStart ReadyMix (Sigma) in the Smart Cycler II Real-Time PCR detection system (Cepheid, Sunnyvale, CA). The primers used were: GAPDH forward, 5′-GGTGGTCTCCTCTG-ACTTCAACA-3′; GAPDH reverse, 5′-GTTGCTGTAGCCAAATTCG-TTGT-3′; V1G1 forward, 5′-GCCGAGAAGGTGTCCGAGGCCCG-3′; V1G1 reverse, 5′-GCGGTACTGTTCAATTTCAGCC-3′; RILP forward, 5′-CGGAAGCAGCGGAAGAAGATCAAG-3′; RILP reverse, 5′-GAG-CAGGATCCATGGGCCAGC-3′. Primers were purchased from Eurofin MWG Operon (Ebersberg, Germany). The PCR program was as follows: 3 min at 94℃; 35 cycles of 30 s at 94℃, 30 s at 60℃ and 30 s at 72℃; and 6 min at 75℃. The specificity of PCR products was checked by performing a melting-curve test.

Acknowledgements

We thank Anna Maria Rosaria Colucci (Novartis Vaccine Institute for Global Health, Siena, Italy) for help in the first two-hybrid screening and Mitsunori Fukuda (Tohoku University, Sendai, Japan) for kindly donating pEF-FLAG-$p150^{Glued}$ plasmid.

Competing interests

The authors declare no competing interests.

Author contributions

M.D.L., L.C., C.P. and V.N. performed experiments. R.P., S.S. and P.P.D.F. provided reagents, expertise and support for the ubiquitylation experiment. M.D.L. and C.B. conceived and designed the experiments and analyzed the results. C.B. wrote the manuscript.

Funding

The financial support of Associazione Italiana per la Ricerca sul Cancro Investigator Grants [grant numbers 10213 and 14709 to C.B.]; Telethon-Italy [grant number GGP09045 to C.B.]; and of Ministero dell'Istruzione, dell'Università e della Ricerca (Projects of significant national interest PRIN 2010–2011 and Basic research funds ex60% to C.B.) is gratefully acknowledged. M.D.L. is a recipient of a triennal Fondazione Italiana per la Ricerca sul Cancro fellowship.

Supplementary material

Supplementary material available online at
http://jcs.biologists.org/lookup/suppl/doi:10.1242/jcs.142604/-/DC1

References

Aloisi, A. L. and Bucci, C. (2013). Rab GTPases-cargo direct interactions: fine modulators of intracellular trafficking. *Histol. Histopathol.* **28**, 839-849.

Aniento, F., Gu, F., Parton, R. G. and Gruenberg, J. (1996). An endosomal β COP is involved in the pH-dependent formation of transport vesicles destined for late endosomes. *J. Cell Biol.* **133**, 29-41.

Armbrüster, A., Bailer, S. M., Koch, M. H., Godovac-Zimmermann, J. and Grüber, G. (2003). Dimer formation of subunit G of the yeast V-ATPase. *FEBS Lett.* **546**, 395-400.

Bartel, P., Chien, C. T., Sternglanz, R. and Fields, S. (1993). Elimination of false positives that arise in using the two-hybrid system. *Biotechniques* **14**, 920-924.

Bucci, C. and Chiariello, M. (2006). Signal transduction gRABs attention. *Cell. Signal.* **18**, 1-8.

Bucci, C., Frunzio, R., Chiariotti, L., Brown, A. L., Rechler, M. M. and Bruni, C. B. (1988). A new member of the ras gene superfamily identified in a rat liver cell line. *Nucleic Acids Res.* **16**, 9979-9993.

Bucci, C., Parton, R. G., Mather, I. H., Stunnenberg, H., Simons, K., Hoflack, B. and Zerial, M. (1992). The small GTPase rab5 functions as a regulatory factor in the early endocytic pathway. *Cell* **70**, 715-728.

Bucci, C., Thomsen, P., Nicoziani, P., McCarthy, J. and van Deurs, B. (2000). Rab7: a key to lysosome biogenesis. *Mol. Biol. Cell* **11**, 467-480.

Cantalupo, G., Alifano, P., Roberti, V., Bruni, C. B. and Bucci, C. (2001). Rab-interacting lysosomal protein (RILP): the Rab7 effector required for transport to lysosomes. *EMBO J.* **20**, 683-693.

Casey, J. R., Grinstein, S. and Orlowski, J. (2010). Sensors and regulators of intracellular pH. *Nat. Rev. Mol. Cell Biol.* **11**, 50-61.

Chavrier, P., Parton, R. G., Hauri, H. P., Simons, K. and Zerial, M. (1990). Localization of low molecular weight GTP binding proteins to exocytic and endocytic compartments. *Cell* **62**, 317-329.

Chiariello, M., Bruni, C. B. and Bucci, C. (1999). The small GTPases Rab5a, Rab5b and Rab5c are differentially phosphorylated in vitro. *FEBS Lett.* **453**, 20-24.

Cipriano, D. J., Wang, Y., Bond, S., Hinton, A., Jefferies, K. C., Qi, J. and Forgac, M. (2008). Structure and regulation of the vacuolar ATPases. *Biochim. Biophys. Acta* **1777**, 599-604.

Clague, M. J., Urbé, S., Aniento, F. and Gruenberg, J. (1994). Vacuolar ATPase activity is required for endosomal carrier vesicle formation. *J. Biol. Chem.* **269**, 21-24.

Cogli, L., Progida, C., Bramato, R. and Bucci, C. (2013a). Vimentin phosphorylation and assembly are regulated by the small GTPase Rab7a. *Biochim. Biophys. Acta* **1833**, 1283-1293.

Cogli, L., Progida, C., Thomas, C. L., Spencer-Dene, B., Donno, C., Schiavo, G. and Bucci, C. (2013b). Charcot-Marie-Tooth type 2B disease-causing RAB7A mutant proteins show altered interaction with the neuronal intermediate filament peripherin. *Acta Neuropathol.* **125**, 257-272.

Colucci, A. M. R., Campana, M. C., Bellopede, M. and Bucci, C. (2005a). The Rab-interacting lysosomal protein, a Rab7 and Rab34 effector, is capable of self-interaction. *Biochem. Biophys. Res. Commun.* **334**, 128-133.

Colucci, A. M. R., Spinosa, M. R. and Bucci, C. (2005b). Expression, assay, and functional properties of RILP. *Methods Enzymol.* **403**, 664-675.

Dautry-Varsat, A., Ciechanover, A. and Lodish, H. F. (1983). pH and the recycling of transferrin during receptor-mediated endocytosis. *Proc. Natl. Acad. Sci. USA* **80**, 2258-2262.

De Luca, A., Progida, C., Spinosa, M. R., Alifano, P. and Bucci, C. (2008). Characterization of the Rab7K157N mutant protein associated with Charcot-Marie-Tooth type 2B. *Biochem. Biophys. Res. Commun.* **372**, 283-287.
Diakov, T. T. and Kane, P. M. (2010). Regulation of V-ATPase activity and assembly by extracellular pH. *J. Biol. Chem.* **285**, 23771-23778.
El Far, O. and Seagar, M. (2011). A role for V-ATPase subunits in synaptic vesicle fusion? *J. Neurochem.* **117**, 603-612.
Forgac, M. (2007). Vacuolar ATPases: rotary proton pumps in physiology and pathophysiology. *Nat. Rev. Mol. Cell Biol.* **8**, 917-929.
Frattini, A., Orchard, P. J., Sobacchi, C., Giliani, S., Abinun, M., Mattsson, J. P., Keeling, D. J., Andersson, A. K., Wallbrandt, P., Zecca, L. et al. (2000). Defects in TCIRG1 subunit of the vacuolar proton pump are responsible for a subset of human autosomal recessive osteopetrosis. *Nat. Genet.* **25**, 343-346.
Harrison, R. E., Bucci, C., Vieira, O. V., Schroer, T. A. and Grinstein, S. (2003). Phagosomes fuse with late endosomes and/or lysosomes by extension of membrane protrusions along microtubules: role of Rab7 and RILP. *Mol. Cell. Biol.* **23**, 6494-6506.
Hernandez, A., Serrano-Bueno, G., Perez-Castineira, J. R. and Serrano, A. (2012). Intracellular proton pumps as targets in chemotherapy: V-ATPases and cancer. *Curr. Pharm. Des.* **18**, 1383-1394.
Hinton, A., Bond, S. and Forgac, M. (2009). V-ATPase functions in normal and disease processes. *Pflugers Arch.* **457**, 589-598.
Hopkins, C. R. and Trowbridge, I. S. (1983). Internalization and processing of transferrin and the transferrin receptor in human carcinoma A431 cells. *J. Cell Biol.* **97**, 508-521.
Hurtado-Lorenzo, A., Skinner, M., El Annan, J., Futai, M., Sun-Wada, G. H., Bourgoin, S., Casanova, J., Wildeman, A., Bechoua, S., Ausiello, D. A. et al. (2006). V-ATPase interacts with ARNO and Arf6 in early endosomes and regulates the protein degradative pathway. *Nat. Cell Biol.* **8**, 124-136.
Johansson, M., Rocha, N., Zwart, W., Jordens, I., Janssen, L., Kuijl, C., Olkkonen, V. M. and Neefjes, J. (2007). Activation of endosomal dynein motors by stepwise assembly of Rab7-RILP-p150^{Glued}, ORP1L, and the receptor betalII spectrin. *J. Cell Biol.* **176**, 459-471.
Jordens, I., Fernandez-Borja, M., Marsman, M., Dusseljee, S., Janssen, L., Calafat, J., Janssen, H., Wubbolts, R. and Neefjes, J. (2001). The Rab7 effector protein RILP controls lysosomal transport by inducing the recruitment of dynein-dynactin motors. *Curr. Biol.* **11**, 1680-1685.
Kane, P. M. (2006). The where, when, and how of organelle acidification by the yeast vacuolar H+-ATPase. *Microbiol. Mol. Biol. Rev.* **70**, 177-191.
Kane, P. M. (2012). Targeting reversible disassembly as a mechanism of controlling V-ATPase activity. *Curr. Protein Pept. Sci.* **13**, 117-123.
Kane, P. M. and Smardon, A. M. (2003). Assembly and regulation of the yeast vacuolar H+-ATPase. *J. Bioenerg. Biomembr.* **35**, 313-321.
Karet, F. E., Finberg, K. E., Nelson, R. D., Nayir, A., Mocan, H., Sanjad, S. A., Rodriguez-Soriano, J., Santos, F., Cremers, C. W., Di Pietro, A. et al. (1999). Mutations in the gene encoding B1 subunit of H+-ATPase cause renal tubular acidosis with sensorineural deafness. *Nat. Genet.* **21**, 84-90.
Kartner, N. and Manolson, M. F. (2012). V-ATPase subunit interactions: the long road to therapeutic targeting. *Curr. Protein Pept. Sci.* **13**, 164-179.
Marshansky, V. and Futai, M. (2008). The V-type H+-ATPase in vesicular trafficking: targeting, regulation and function. *Curr. Opin. Cell Biol.* **20**, 415-426.
Murata, Y., Sun-Wada, G. H., Yoshimizu, T., Yamamoto, A., Wada, Y. and Futai, M. (2002). Differential localization of the vacuolar H+ pump with G subunit isoforms (G1 and G2) in mouse neurons. *J. Biol. Chem.* **277**, 36296-36303.
Ohbayashi, N., Yatsu, A., Tamura, K. and Fukuda, M. (2012). The Rab21-GEF activity of Varp, but not its Rab32/38 effector function, is required for dendrite formation in melanocytes. *Mol. Biol. Cell* **23**, 669-678.
Ohira, M., Smardon, A. M., Charsky, C. M., Liu, J., Tarsio, M. and Kane, P. M. (2006). The E and G subunits of the yeast V-ATPase interact tightly and are both present at more than one copy per V1 complex. *J. Biol. Chem.* **281**, 22752-22760.
Pérez-Sayáns, M., Somoza-Martín, J. M., Barros-Angueira, F., Rey, J. M. and García-García, A. (2009). V-ATPase inhibitors and implication in cancer treatment. *Cancer Treat. Rev.* **35**, 707-713.
Pietrement, C., Sun-Wada, G. H., Silva, N. D., McKee, M., Marshansky, V., Brown, D., Futai, M. and Breton, S. (2006). Distinct expression patterns of different subunit isoforms of the V-ATPase in the rat epididymis. *Biol. Reprod.* **74**, 185-194.
Progida, C., Spinosa, M. R., De Luca, A. and Bucci, C. (2006). RILP interacts with the VPS22 component of the ESCRT-II complex. *Biochem. Biophys. Res. Commun.* **347**, 1074-1079.
Progida, C., Malerød, L., Stuffers, S., Brech, A., Bucci, C. and Stenmark, H. (2007). RILP is required for the proper morphology and function of late endosomes. *J. Cell Sci.* **120**, 3729-3737.
Progida, C., Cogli, L., Piro, F., De Luca, A., Bakke, O. and Bucci, C. (2010). Rab7b controls trafficking from endosomes to the TGN. *J. Cell Sci.* **123**, 1480-1491.
Qi, J., Wang, Y. and Forgac, M. (2007). The vacuolar (H+)-ATPase: subunit arrangement and in vivo regulation. *J. Bioenerg. Biomembr.* **39**, 423-426.
Qiu, Q. S. (2012). V-ATPase, ScNhx1p and yeast vacuole fusion. *J. Genet. Genomics* **39**, 167-171.
Roxrud, I., Raiborg, C., Gilfillan, G. D., Strømme, P. and Stenmark, H. (2009). Dual degradation mechanisms ensure disposal of NHE6 mutant protein associated with neurological disease. *Exp. Cell Res.* **315**, 3014-3027.
Sennoune, S. R. and Martinez-Zaguilan, R. (2012). Vacuolar H(+)-ATPase signaling pathway in cancer. *Curr. Protein Pept. Sci.* **13**, 152-163.
Sennoune, S. R., Bakunts, K., Martínez, G. M., Chua-Tuan, J. L., Kebir, Y., Attaya, M. N. and Martínez-Zaguilán, R. (2004a). Vacuolar H+-ATPase in human breast cancer cells with distinct metastatic potential: distribution and functional activity. *Am. J. Physiol.* **286**, C1443-C1452.
Sennoune, S. R., Luo, D. and Martínez-Zaguilán, R. (2004b). Plasmalemmal vacuolar-type H+-ATPase in cancer biology. *Cell Biochem. Biophys.* **40**, 185-206.
Smardon, A. M., Tarsio, M. and Kane, P. M. (2002). The RAVE complex is essential for stable assembly of the yeast V-ATPase. *J. Biol. Chem.* **277**, 13831-13839.
Smith, A. N., Skaug, J., Choate, K. A., Nayir, A., Bakkaloglu, A., Ozen, S., Hulton, S. A., Sanjad, S. A., Al-Sabban, E. A., Lifton, R. P. et al. (2000). Mutations in ATP6N1B, encoding a new kidney vacuolar proton pump 116-kD subunit, cause recessive distal renal tubular acidosis with preserved hearing. *Nat. Genet.* **26**, 71-75.
Spinosa, M. R., Progida, C., De Luca, A., Colucci, A. M. R., Alifano, P. and Bucci, C. (2008). Functional characterization of Rab7 mutant proteins associated with Charcot-Marie-Tooth type 2B disease. *J. Neurosci.* **28**, 1640-1648.
Stenmark, H. (2009). Rab GTPases as coordinators of vesicle traffic. *Nat. Rev. Mol. Cell Biol.* **10**, 513-525.
Sun-Wada, G. H., Wada, Y. and Futai, M. (2004). Diverse and essential roles of mammalian vacuolar-type proton pump ATPase: toward the physiological understanding of inside acidic compartments. *Biochim. Biophys. Acta* **1658**, 106-114.
Suter, B., Kittanakom, S. and Stagljar, I. (2008). Two-hybrid technologies in proteomics research. *Curr. Opin. Biotechnol.* **19**, 316-323.
Toei, M., Saum, R. and Forgac, M. (2010). Regulation and isoform function of the V-ATPases. *Biochemistry* **49**, 4715-4723.
Tomashek, J. J., Graham, L. A., Hutchins, M. U., Stevens, T. H. and Klionsky, D. J. (1997). V1-situated stalk subunits of the yeast vacuolar proton-translocating ATPase. *J. Biol. Chem.* **272**, 26787-26793.
Toyomura, T., Murata, Y., Yamamoto, A., Oka, T., Sun-Wada, G. H., Wada, Y. and Futai, M. (2003). From lysosomes to the plasma membrane: localization of vacuolar-type H+ -ATPase with the a3 isoform during osteoclast differentiation. *J. Biol. Chem.* **278**, 22023-22030.
Trajkovic, K., Hsu, C., Chiantia, S., Rajendran, L., Wenzel, D., Wieland, F., Schwille, P., Brügger, B. and Simons, M. (2008). Ceramide triggers budding of exosome vesicles into multivesicular endosomes. *Science* **319**, 1244-1247.
Vitelli, R., Santillo, M., Lattero, D., Chiariello, M., Bifulco, M., Bruni, C. B. and Bucci, C. (1997). Role of the small GTPase Rab7 in the late endocytic pathway. *J. Biol. Chem.* **272**, 4391-4397.

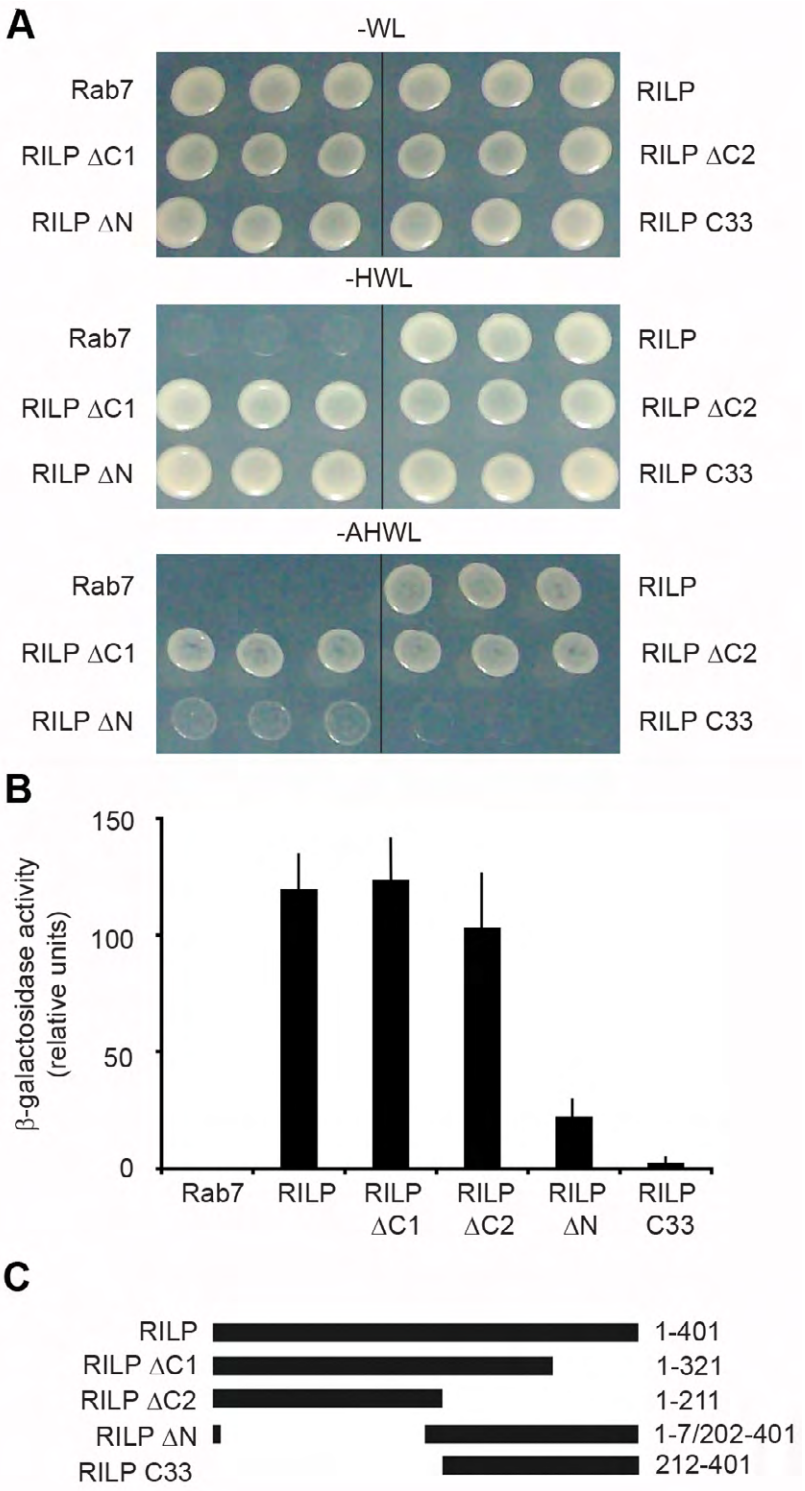

Fig. S1. Interaction between RILP and the V1G1 subunit of the V-ATPase in the two-hybrid system. AH109 yeast cells were co-transformed with pGADT7-V1G1 and pGBKT7, PGBKT7-Rab7, PGBKT7-RILPwt or mutant constructs as indicated. (**A**) Three independent colonies for each double transformation were plated on WL and HWL synthetic medium and grown at 30 °C for three days. (**B**) The β-galactosidase activity of double transformants was measured using o-nitrophenyl-β-D-galactoside as substrate as detailed in Materials and methods. Activities are measured as arbitrary relative units and represent mean ± s.d. values of 9 independent transformants from three independent experiments. (**C**) Scheme depicting the different RILP deletion mutants used. One the right side of the panel the amino acids included in the mutant proteins are indicated.

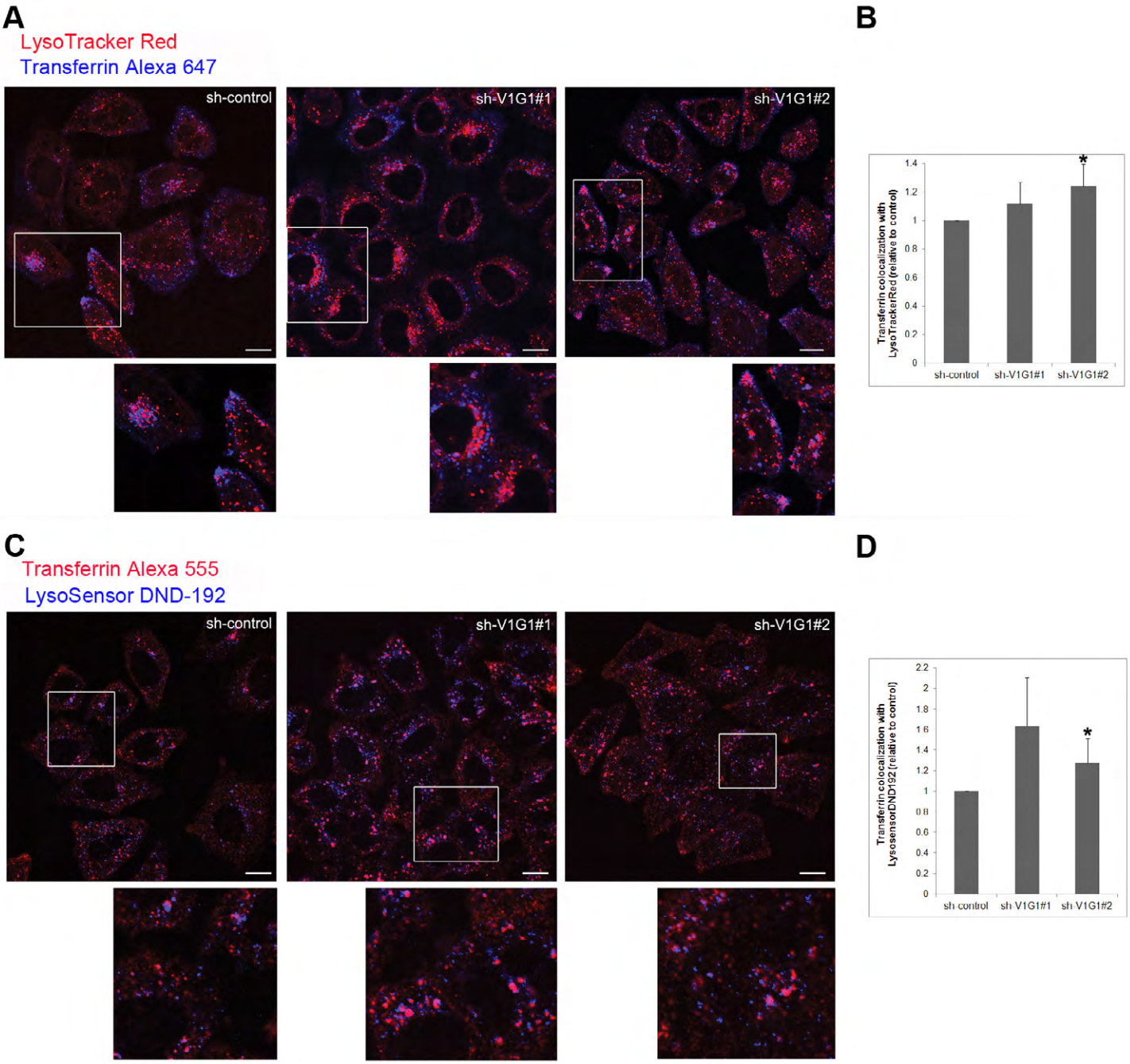

Fig. S2. V1G1 depletion affects transferrin distribution. HeLa cells expressing stably (clones 1 and 2) sh-V1G1 or control RNA (sh-control) were incubated with LysoTracker Red and Alexa 647-transferrin for 30 min. Cells were analyzed by live microscopy (**A**), and the relative level of transferrin colocalizing with LysoTracker was quantified (**B**). HeLa cells expressing stably (clones 1 and 2) sh-V1G1 or control RNA (sh-control) were incubated with LysoSensor DND-192 and Alexa 555-transferrin for 30 min. Cells were analyzed by live microscopy (**C**), and the relative level of transferrin colocalizing with LysoSensor was quantified (**D**). For each image, magnifications of the boxed areas are shown in the respective lower insets. Bar = 10 μm. Histograms represent the average (± s.e.m.) of two independent experiments where at least 50 cells were quantified per experiment.